High-Speed Surfactant-Free Fabrication of Large Carbon Nanotube Membranes for Multifunctional Composites

Siddhant Datta[1]; Masoud Yekani Fard[2]; and Aditi Chattopadhyay[3]

Abstract: A high-speed manufacturing process for multiwalled carbon nanotube (MWNT) buckypaper is presented, and its application as an embedded strain sensor for composite materials is demonstrated. This manufacturing method enables the production of sizable carbon nanotube (CNT) membranes with significantly reduced processing time and less manufacturing complexity than other contemporary techniques. The use of surfactants and chemical functionalization of MWNTs was completely avoided in this method because functionality of carbon nanotubes can be hampered by such surface treatments. Microstructure, mechanical properties, and piezoresistive response of the fabricated buckypaper were characterized, and its sensitivity as a strain sensor was analyzed. Stable piezoresistive response could be achieved at low strains, and a high sensitivity to strain was observed when buckypaper was embedded in glass fiber epoxy laminates for strain sensing.
DOI: 10.1061/(ASCE)AS.1943-5525.0000558.

Introduction

Since the discovery of carbon nanotubes (CNTs) by Iijima (1991), they have gained immense popularity in the field of nanocomposites by exhibiting an unprecedented combination of beneficial mechanical, thermal, and electrical properties. The use of CNTs as nanofiller in polymer composites has shown considerable improvement in mechanical properties such as tensile and compressive strength, elastic modulus, and fatigue resistance in addition to enhanced thermal and electrical properties (Thostenson et al. 2001; Chen et al. 2008; Cheng et al. 2009; Ashrafi et al. 2010). Recently, polymer/CNT nanocomposites have received extensive recognition for their versatility in a variety of applications such as water purification, gas sensing, strain sensing, super capacitance, fuel cell electrodes, fire-retardant coatings, artificial muscles, EMI shielding, and self-heating hybrid composites for deicing (Dumée et al. 2010; Slobodian et al. 2011; Benlikaya et al. 2013; Kang et al. 2006; Zheng et al. 2013; Zhu et al 2010; Fu et al. 2010; Park 2009; Chu et al. 2014; Vohrer et al. 2004). These applications use CNTs in the form of buckypaper, which is a thin porous membrane of highly entangled CNTs held together by van der Waals forces.

Vacuum filtration is the current method used by many researchers for manufacturing buckypaper (Dumée et al. 2010; Slobodian et al. 2011; Benlikaya et al. 2013; Kang et al. 2006; Zheng et al. 2013; Zhu et al 2010; Fu et al. 2010; Park 2009; Chu et al. 2014; Vohrer et al. 2004; Rein et al. 2011; Dharap et al. 2004). This method involves vacuum-assisted filtration of a homogeneously dispersed CNT solution using a polytetrafluoroethylene (PTFE) or nylon filter with submicron-sized pores. CNTs are deposited on the filter surface and form a thin membrane (i.e., buckypaper) that can be lifted off the filter surface after drying. Dumee et al. (2010) developed a buckypaper membrane for water purification using the vacuum filtration manufacturing method. This technique has been used for manufacturing buckypaper membranes as an embedded strain sensor in epoxy dog-bone specimens by Rein et al. (2011), as a smart skin for strain sensing in aircraft wings by Dharap et al. (2004), and as a deicing glass fiber–reinforced polymer (GFRP) nanocomposite by Chu et al. (2014). The implementation of most of these nascent ideas has been limited to laboratory scale because of the size limitations imposed by the current fabrication methods for buckypaper. A more rapid, large-scale manufacturing technique is critical to extend the application of these multifunctional capabilities to industrial scale.

Vacuum filtration method limits the size of the manufactured buckypaper to the diameter of the filter used and can lead to heterogeneous distribution of CNT bundles in the finished product (Yeh 2004). Using filters with larger diameters may not completely solve the issue because it would require large volumes of CNT solution to be filtered. Maintaining homogeneous dispersion in a large volume of CNT solution is a challenging task due to the tendency of CNTs to form agglomerates/clusters. Filtering larger quantities of solution through submicron filters can take several hours, depending on the diameter and pore size of the filter, volume of solution filtered, and the pressure difference applied by a vacuum pump. Another disadvantage of this method is the need for surfactants or chemical functionalization of CNTs to assist in obtaining a stable uniform dispersion during filtration (Islam et al. 2003; Ounnunkad et al. 2011). Following filtration, the surfactants can be difficult to remove from the buckypaper and can hamper the efficiency of the membrane for applications such as water purification, gas separation, and biofuel cell electrodes (Rein et al. 2011). Chemical modification of CNTs prior to the filtration can also degrade the functionality of buckypaper for the aforementioned applications (Lin 2005; Liu et al. 2013; Tasis et al. 2003; Sears et al. 2010). Another fabrication method for CNT membranes, which is not commonly used by researchers possibly due to its complexity, is hydroentanglement developed by Zhang (2008). This method involves impregnation of high-speed water jets onto CNTs present on a porous substrate. The CNTs get highly entangled due to the high pressure of water jets, but this process requires high power consumption and has a complex setup, limiting its capability to smaller size membranes. A method for manufacturing continuous strips of buckypaper was developed by Young (2009) using a

[1]Graduate Student, Dept. of Mechanical and Aerospace Engineering, Arizona State Univ., Tempe, AZ 85287 (corresponding author). E-mail: sdatta10@asu.edu

[2]Assitant Research Professor, Dept. of Mechanical and Aerospace Engineering, Arizona State Univ., Tempe, AZ 85287.

[3]Regents' Professor, Dept. of Mechanical and Aerospace Engineering, Arizona State Univ., Tempe, AZ 85287.

Note. This manuscript was submitted on April 25, 2015; approved on July 24, 2015; published online on September 30, 2015. Discussion period open until February 29, 2016; separate discussions must be submitted for individual papers. This paper is part of the ***Journal of Aerospace Engineering***, © ASCE, ISSN 0893-1321.

continuous 38.1-mm (1.5-in.)-wide filter made of acrylonitrile butadiene styrene (ABS) plastic. The method shows good potential for manufacturing continuous buckypaper strips. However, the design complexities of the vacuum filtration system used in this method lead to longer processing time and fabrication of wider, continuous buckypaper membranes could be a challenging task. Recently, a slurry-based fabrication process, with a few similarities to the proposed method in this paper, was developed by Veliky (2014). This method used CNT/paraffin wax slurry produced through sonication to form molds from which paraffin wax could be extracted. A vacuum-bagging method was used to obtain thin CNT membranes by pushing out the paraffin wax and thin membranes could be obtained. Nevertheless, CNT membranes did not have a completely smooth surface finish, and larger CNT membranes would require bigger vacuum-bagging setups and higher power consumption.

In this paper, a novel fabrication method is presented that facilitates the production of significantly larger buckypapers than would be possible with current manufacturing techniques. The thickness of the membranes can be controlled ranging from 150 to 1,300 μm. This method does not require the use of surfactant-assisted dispersion, chemical functionalization, or the use of any filtration technique; hence, processing time can be reduced by approximately six to eight times depending upon the size of buckypaper membrane. Unlike the current technique in which some fraction of CNTs passed through filtration membrane, there is no wastage of CNTs in the proposed method. This technique provides the potential to advance buckypaper from laboratory-scale demonstrations to industrial-scale applications because there is no size limitation for the buckypaper membrane. Various properties of the buckypaper membranes such as microstructure, structural homogeneity and properties, electrical conductivity, BET specific surface area (SSA), and pore-size distribution were investigated. The piezoresistive property was exploited to demonstrate its applicability as an embedded strain sensor in a glass-fiber epoxy composite.

Fabrication and Characterization of a Large-Size Buckypaper Membrane

Multiwalled carbon nanotubes used in this research were obtained from US Research Nanomaterials (Houston, Texas) and produced using the chemical vapor deposition (CVD) technique. The CNT average outer diameter was 10–30 nm with an average length of 15–30 μm. Purity of the MWNTs was confirmed to be 90% as claimed by the supplier. Fig. 1 shows the schematic steps of the proposed manufacturing technique. A volume of 5 mL of high-concentration solution (25 mg/mL) of MWNTs in methanol is required to fabricate a buckypaper of approximately 4.4-cm diameter with an average thickness of 200 μm. The high-concentration solution was ultrasonicated with a tip sonicator, leading to the evaporation of methanol solvent, until a highly viscous slurry of MWNTs and methanol was obtained. This slurry was stirred with a glass rod to improve homogeneity and laid up for compression between two steel plates. Steel plates were covered with plastic sheets to avoid adhesion between the buckypaper and the compression plates. For a buckypaper of approximately 4.4-cm diameter, the slurry was laid down in a circular disk shape with a diameter of approximately 2.5 cm and thickness of approximately 3 mm. A 20-t hydraulic press was used to compress the slurry into a thin membrane. Compressing the MWNT/methanol slurry into a thin membrane should be performed at a very slow rate to prevent the methanol from gushing out and creating cracks. The two plates sandwiching the membrane are then unmounted from the press and placed into an oven at 60°C for 1 h. After drying, the top plate was removed, and the free-standing MWNT buckypaper was degassed for 24 h. Once the process was finalized, the capability of this novel fabrication procedure to make larger buckypapers was proven by using a greater quantity of MWNT/methanol slurry for a single buckypaper. The thickness of the buckypaper can be controlled by changing the wetness of the slurry and the load applied by the hydraulic press. Higher methanol content in the slurry reduces the required force for compression, and thinner buckypapers can be obtained with relatively less compressing force. The minimum thickness of buckypaper achieved through this fabrication process, with the hydraulic press loaded to full capacity, was approximately 100 μm. Fig. 2 shows a large-size (20 × 16 cm) free-standing buckypaper with stable structure and smooth surface finish fabricated by scaling up the quantity of MWNT/methanol during fabrication.

Buckypapers obtained from this technique showed uniform thickness and a robust structure with an average density of 0.42 g/cc, which is close to the density of buckypapers fabricated

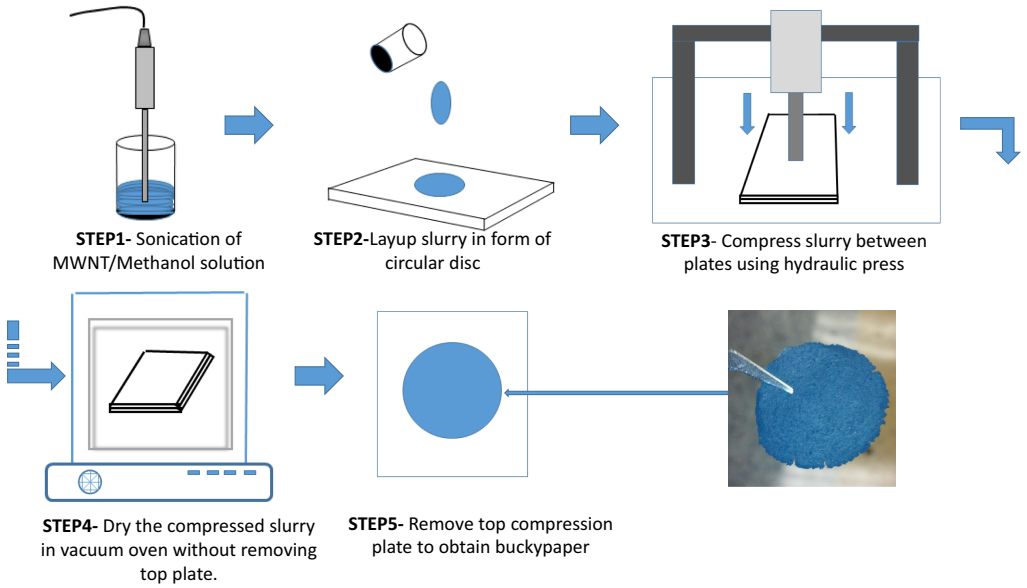

Fig. 1. Schematic of buckypaper manufacturing process

J. Aerosp. Eng., 2016, 29(3): 04015060

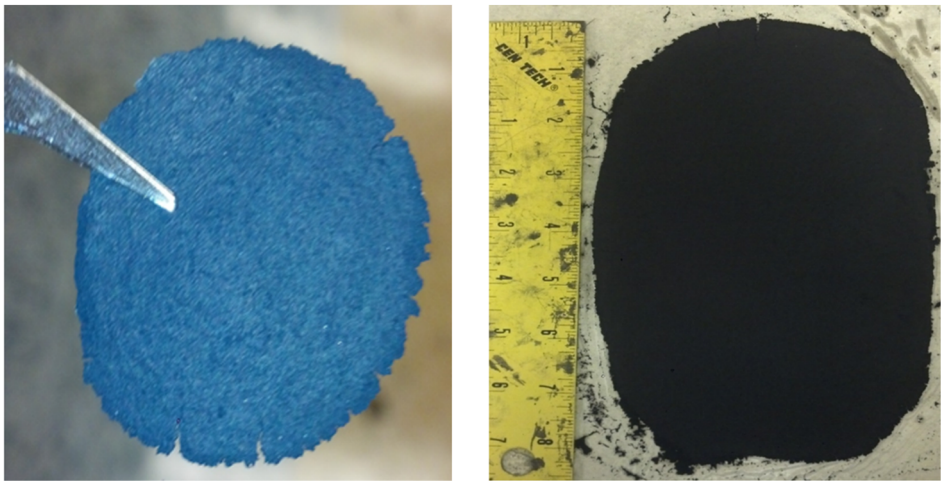

(a) (b)

Fig. 2. (a) Free-standing buckypaper lifted off the compression plate; (b) 20 × 16-cm buckypaper manufactured by scaling up quantity of methanol/MWNT slurry

by the vacuum filtration technique (Lin 2005; Zhang and Jiang 2012). Qualitative analysis of buckypapers made using this novel method was performed using a JEOL XL-30 scanning electron microscope (SEM) (Tokyo, Japan). Morphology and surface quality of the buckypapers were analyzed from SEM scans starting with low magnification and progressing to higher magnification levels. SEM micrographs of buckypaper cross section were obtained at different locations along the width to determine the degree of uniformity in thickness. Fig. 3(a) is a low-magnification SEM image (15,000×) showing a uniform, crack-free, and stable structure composed of highly entangled MWNTs. Uniformly distributed and randomly oriented MWNT bundles and the absence of large voids [Figs. 3(a and b)] suggest homogeneity in microstructure and isotropic material properties. Two types of pores were observed in the SEM micrographs of buckypaper and are marked with black and white arrows in Fig. 3(c). The first type is the intrabundle pore (marked with black arrows), which is present within a CNT bundle. The second type is the interbundle pore (marked with white arrows), which is present between CNT bundles. The uniformity in thickness evaluated using SEM micrographs of buckypaper cross section is depicted in Fig. 4. The average and standard deviation of thickness of the membrane shown in Fig. 4 were found to be 242.06 and 7.86 μm, respectively.

The direct current (DC) electrical resistance of buckypaper was measured at room temperature with a digital multimeter (Fluke 189), using the two-probe method. The 3 × 1-cm buckypaper strips were used for conductivity measurements and 0.5 cm at each end was painted with silver paint to form electrodes, leaving 2 cm of effective length in the middle. The DC conductivity (σ) of buckypapers and buckypaper/epoxy films was calculated at room temperature from the following relationship (Dieze-Pascual et al. 2012)

$$\sigma = \frac{L}{AR} \tag{1}$$

where L = effective length of specimen between electrodes; A = cross-sectional area; and R = measured DC resistance value from the multimeter. The average electrical conductivity of buckypapers was 1.32×10^4 S/m. After being impregnated with epoxy to form the nanocomposite films the conductivity value dropped to 2.12×10^{-4} S/m.

N2 adsorption–desorption isotherms were collected at 77 K using a Micrometrics Tristar II 3020 surface area and porosity analyzer (Norcross, Georgia). SSA was obtained by the BET technique, whereas the pore-size distribution and cumulative pore content were obtained by the Barrett-Joyner-Halenda (BJH) method (Zhang and Jiang 2012).

The BET SSA, as obtained from N2 adsorption isotherms of six different samples of buckypaper, was in the range of 94.62–107.20 m^2/g with the average value of 102.60 m^2/g. The SSA of CNTs in their original powder form was 200 m^2/g, thus high SSA was retained in the buckypaper form. High SSA is a desirable property for a variety of applications such as fuel cell electrodes, gas/vapor sensing, catalyst, water purification, and high weight fraction nanocomposites (Lopes et al. 2010). The pore-size distribution obtained from BJH analysis for the buckypaper specimen with maximum SSA of 107.20 m^2/g is presented in Fig. 5. This plot is useful for comparing the relative pore volumes between pore-size range as the apparent area under the curve is directly proportional to the real volume occupied by pores in that size range. The plot of $dV/d\log(W)$ versus W reveals that pores ranging from 70 to 120 nm in size occupy relatively larger volume than the micropore ($\cong$1.7–4 nm), mesopore ($\cong 10-40$ nm), and large-size (120–250 nm) macropores. The peak observed in the size range of 70–120 nm represents pores between CNT bundles (i.e., interbundle pores). The very local sharp peak corresponding to the pore-size range of 20–30 nm is associated with the presence of intrabundle pores, because these pores generally have dimensions close to average CNT diameter (Zhang and Jiang 2012; Dieze-Pascual et al. 2012). A set of micropores at 1.7–4 nm was observed in pore volume plots due to intertube channels between adjacent MWNTs and smaller intrabundle pores (Pham et al. 2008). Specific surface area distribution as a function of pore width is also presented in Fig. 5. It can be seen from this plot that, while the pore volumes are mainly associated with midsized macropores, the SSA is dominated by micropores (intertube channels and smaller intrabundle pores) of 1.7–4-nm width providing an indication of their higher concentration. The total porosity (Φ) was calculated from the relationship (Zhang and Jiang 2012)

$$\Phi = 1 - \rho_{bp}/\rho_{cnt} \tag{2}$$

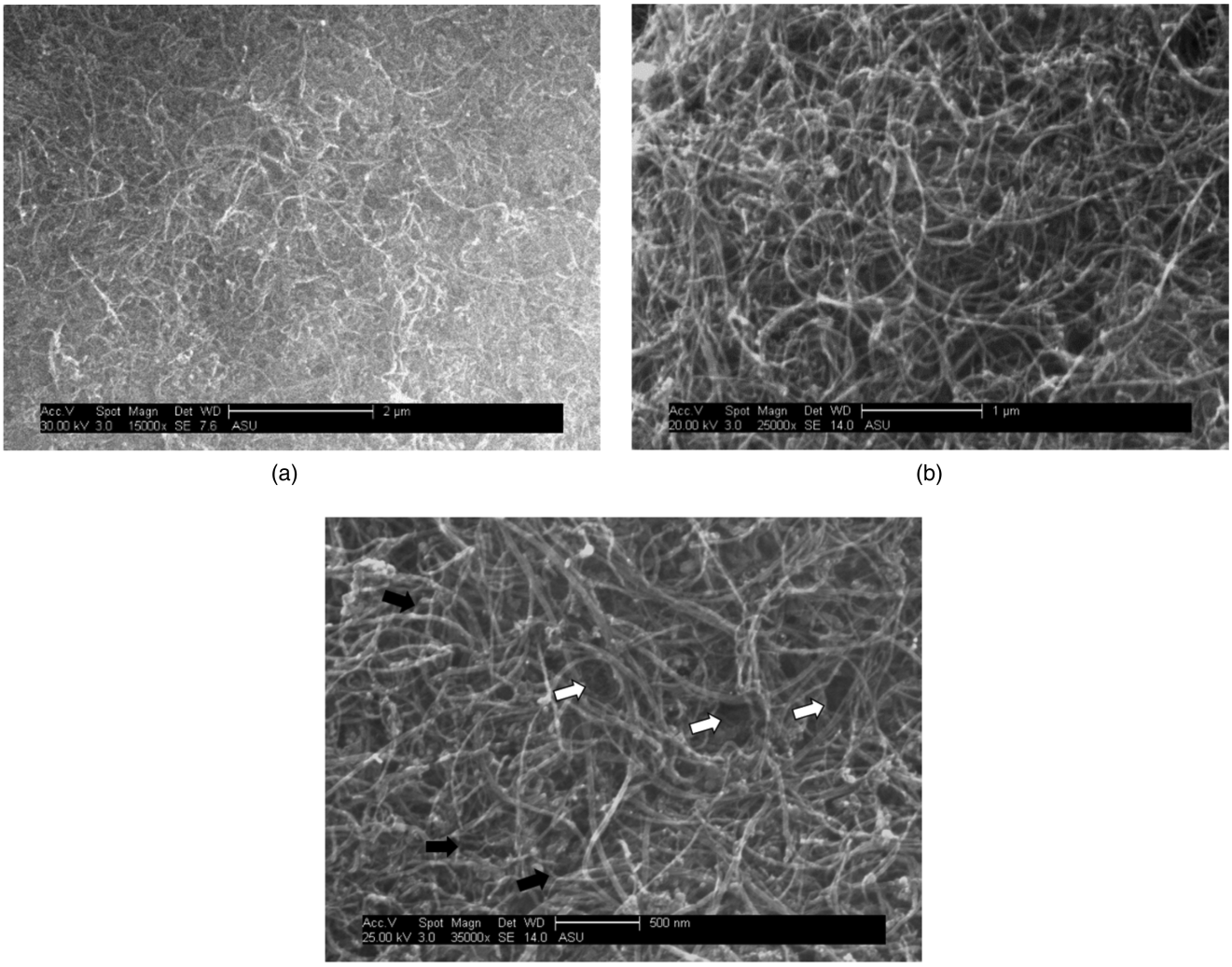

Fig. 3. SEM micrographs for buckypaper showing interbundle and intrabundle pores: (a) 15,000×; (b) 25,000×; (c) 35,000×

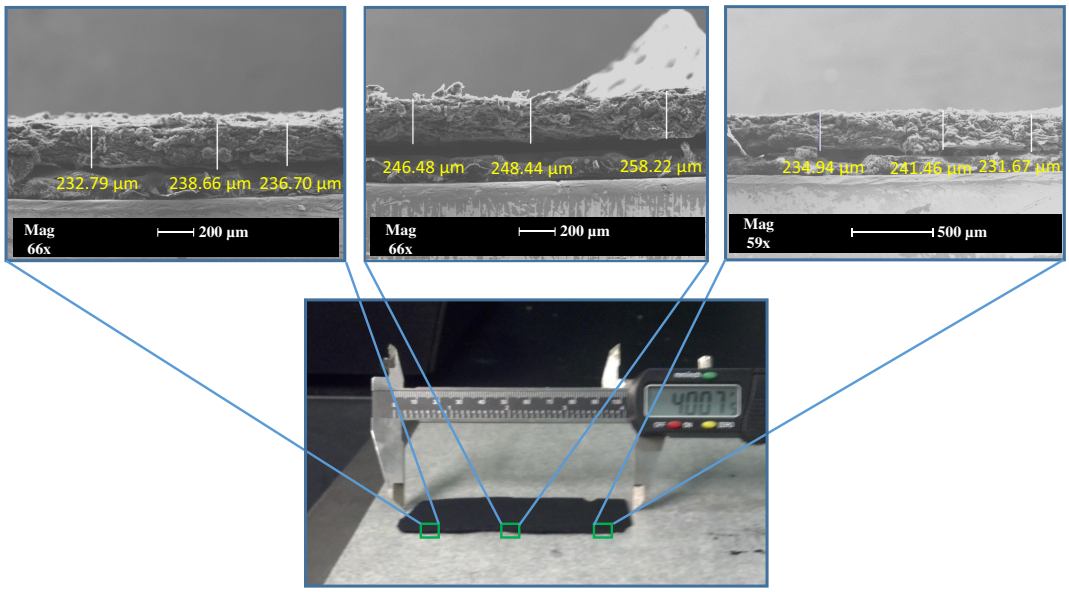

Fig. 4. Uniformity in thickness across the width of 10.2-cm (4-in.)-wide buckypaper specimen

J. Aerosp. Eng., 2016, 29(3): 04015060

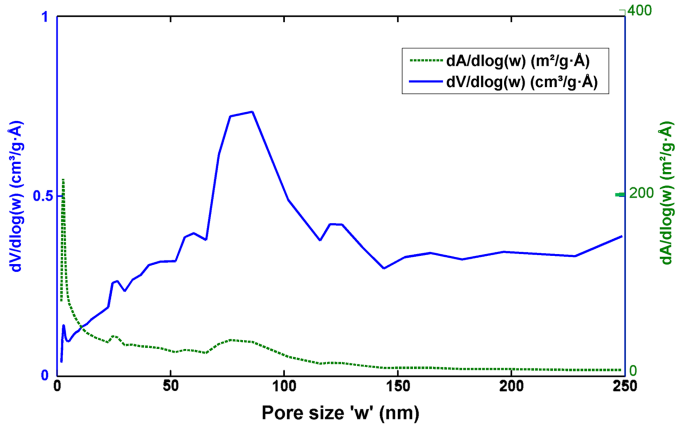

Fig. 5. Pore-size distribution as derivative plot of pore volume with respect to pore width versus pore width (solid line) and surface area distribution as derivative plot of surface area with respect to pore width versus pore width (dashed line)

where ρ_{bp} = bulk density of buckypaper; and ρ_{cnt} = density of MWNTs (2.1 g/mL). The total porosity was in the range of 76.3–84.4% with an average value of 81%. In the following sections, the strain-sensing capability and the mechanical properties of buckypaper-based nanocomposites are presented.

Fabrication and Characterization of Self-Sensing GFRP Hybrid Composites

Eight-harness satin (8HS) weave of S2 glass fiber from Fibre Glast (Brookville, Ohio) and thermoset epoxy resin Epon 863 with hardener EPI-CURE 3290 with a 100/27 weight ratio, provided by FiberglassSite (Edgewood, Maryland), were used to fabricate the self-sensing GFRP laminates using the wet layup method. The six-layer composite laminates were cured at room temperature for 7 days. The laminate was cut into 20.3 × 2.5-cm (8 × 1-in). strips for tensile tests. Buckypaper was embedded in the center layer (between the third and the fourth lamina), spanning the gauge length, while laying up the laminate. Tensile tests were conducted on self-sensing GFRP specimens at a constant displacement rate of 0.5 mm/min on an MTS Bionix servohydraulic test system. Under monotonic tensile loading, the piezoresistive response of buckypaper-embedded GFRP laminates was recorded using the Fluke 289 multimeter with a data-logging feature and the strain fields on the specimen surface were analyzed using a Digital Image Correlation (DIC) ARAMIS 5M system (ARAMIS 2012). Sensitivity, also known as gauge factor, of the buckypaper sensors was calculated from the relation (Oliva-Aviles et al. 2011)

$$GF = \left(\frac{R - R_o}{R_o}\right)\left(\frac{1}{\varepsilon}\right) \tag{3}$$

where R = electrical resistance at strained state; R_o = original resistance; and ε = longitudinal strain increment. Strain distribution in the buckypaper-embedded region of the GFRP specimens, obtained from DIC, is shown in Figs. 6(a and b). Strains along the loading axis are shown at intermediate and failure stages in Figs. 6(a and b), respectively. Reasonably uniform strain distribution was observed until approximately 1% average strain and the sensor data directly correlates with the average global strain until this point. At average strain greater than 1%, the strain distribution starts to become nonuniform and sensor data cannot be considered to represent average strain in the region between electrodes. Piezoresistive response of the buckypaper-embedded GFRP strips under tensile loading is presented in Fig. 7. Fig. 7(a) shows the normalized resistance change as the strain evolves until failure. Fig. 7(b) shows stable sensitivity of the embedded buckypaper until 1.3% strain. The average sensitivity of five self-sensing GFRP specimens as calculated by a linear fit between 0.2 and 0.6% strain was found to be 4.21. This is significantly higher than sensitivity values reported in literature for many CNT-based sensors (Rein et al. 2011; Meng et al. 2008; Bautista-Quijano et al. 2010). It is also greater than the

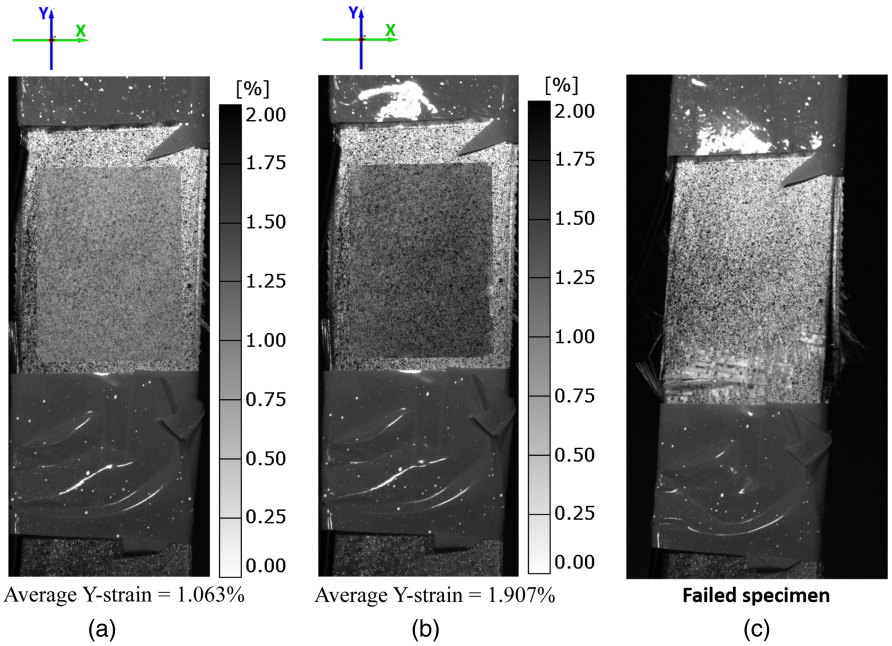

Fig. 6. (a) Uniform strain distribution in buckypaper embedded region until 1% strain; (b) strain distribution on specimen surface just before failure; (c) failed specimen

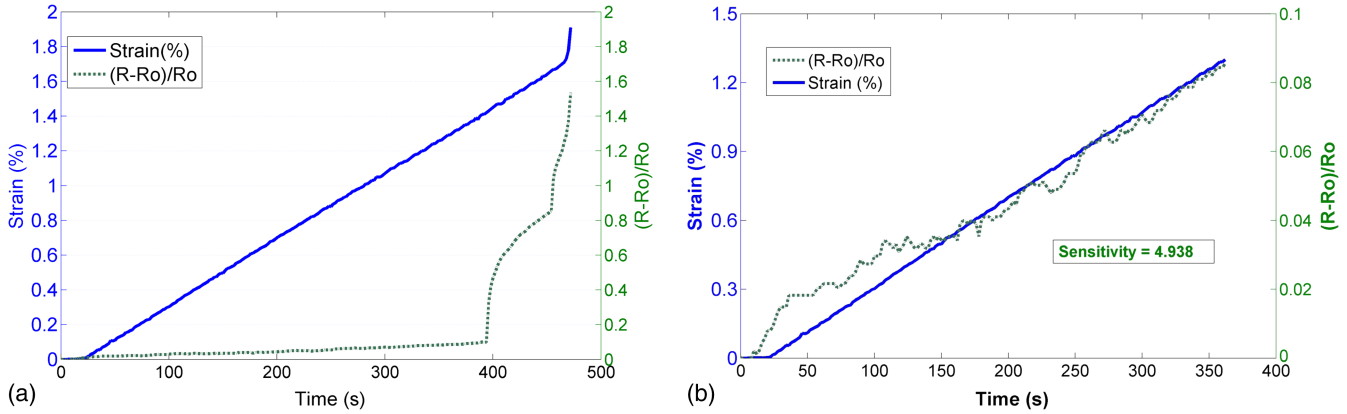

Fig. 7. (a) Piezoresistive response of the buckypaper-embedded GFRP until failure; (b) until 1.3% strain showing stable sensitivity

sensitivity for commercially available conventional strain gauges. Higher sensitivity is clearly desirable, allowing very low strains to be detected with a measurable resistance change.

Fabrication and Mechanical Characterization of Nanocomposite Films

Thermoset epoxy resin PRI2002-3-R-A and hardener PRI2000-5-HR-B with a 100/22 weight ratio, provided by PRI (Phoenix, Arizona), was used in the fabrication of nanocomposites films. For the fabrication of buckypaper/epoxy nanocomposite films with high MWNT content, buckypaper was sandwiched between two rectangular pieces of bleeder cloth, and resin was poured over the bleeder cloth surface and spread using a hand layup tool. This layup technique forced the resin through the porous cloth, allowing it to permeate into the porous buckypaper. Both sides of the buckypaper were impregnated using this layup method and specimens were cured for 12 h at 65°C. The process for resin impregnation was not vacuum assisted to avoid any alteration of the buckypaper's MWNT network, because resin penetration under higher pressure can lead to displacement of CNT bundles. The average thickness for buckypaper/epoxy films was approximately 800 μm. The quality of resin impregnation in buckypaper/epoxy nanocomposites was determined by cross-sectional examination using SEM. Randomly dispersed CNT and pristine specimens were also fabricated for comparison of mechanical properties. A concentration of 1% by weight randomly dispersed MWNT/epoxy was fabricated by first sonicating MWNTs in epoxy using a tip sonicator for 1 h and stopping at intervals of 10 min to manually stir the mixture with a glass rod. The mixture of randomly dispersed MWNTs and epoxy was cast into films by solution casting. The average thickness of pristine epoxy and MWNT/epoxy films was approximately 500 μm. Tensile tests on the films were conducted using a desktop Test Resources load frame manufactured at Shakopee, Minnesota. The tests were performed at a displacement rate of 0.0063 mm/s. The strain response of the films under tension was analyzed using a DIC system. DIC has been widely used for studying strain fields in various engineering and material science problems (Yekani Fard et al. 2012a, b, 2014a, b; Moerman et al. 2009). As a result of the

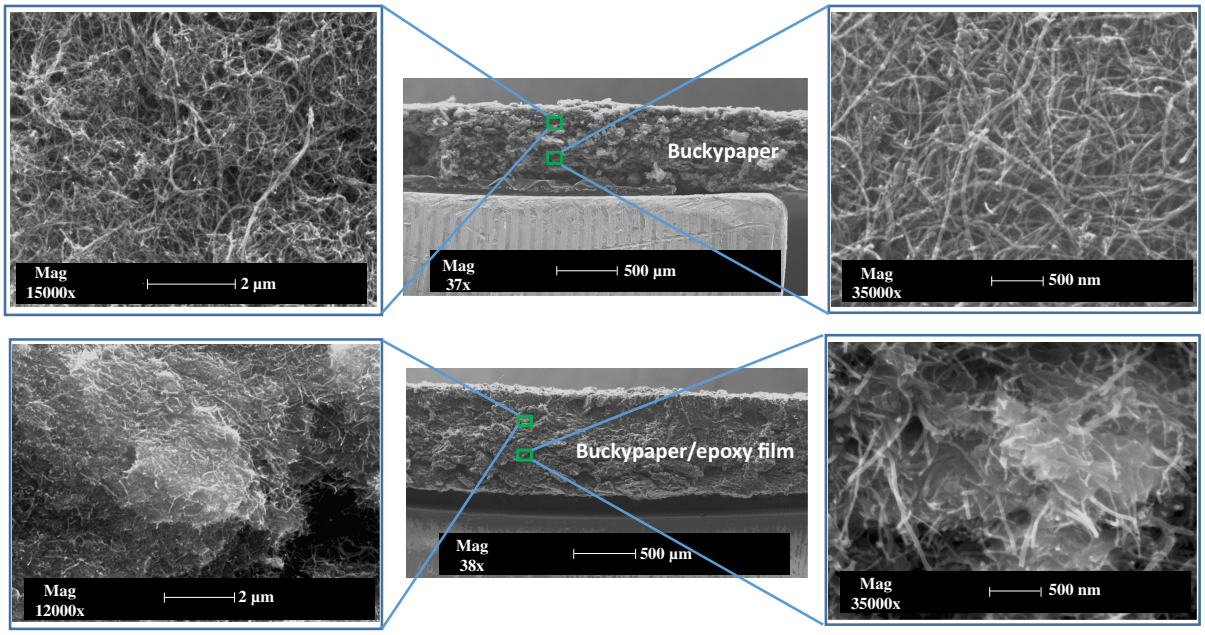

Fig. 8. Evaluation of through-thickness resin impregnation quality using SEM

J. Aerosp. Eng., 2016, 29(3): 04015060

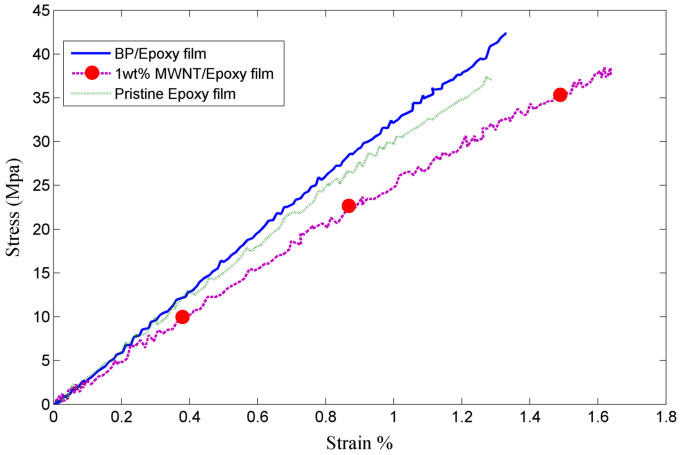

Fig. 9. Stress–strain curves of polymer films with 0, 1, and 30% by weight MWNTs

fabrication procedure, buckypaper/epoxy films with a high MWNT content of 26–30% by weight could be obtained. Fig. 8 shows SEM micrographs of buckypaper/epoxy film cross sections for the assessment of resin impregnation quality. For comparison, SEM micrographs of neat buckypaper cross section are also shown in Fig. 8 to facilitate the evaluation of resin impregnation quality. Areas for analysis were picked from the low-magnification cross-sectional image (38×) and are represented by small green boxes. High-magnification SEM images of buckypaper/epoxy films at different depths from the top surface reveal full penetration of the resin through the thickness of buckypaper and good impregnation quality (Cooper et al. 2003; Whitby et al. 2008). Stress–strain response of polymer films under tensile loading was analyzed to better understand the interfacial interaction/adhesion between epoxy resin and the embedded CNTs. Stress–strain curves of representative specimens for pristine and nanofilled epoxy films under tensile loading are shown in Fig. 9. The average mechanical properties with standard deviations obtained from five specimens are presented in Table 1. Strains obtained from DIC were used to plot the stress–strain curves to analyze mechanical properties accurately. Buckypaper/epoxy films exhibited 20% greater Young's modulus when compared with pristine epoxy films. This can be attributed to good resin penetration and strong interfacial interaction between resin and CNTs of the reinforcing buckypaper. Higher Young's modulus indicates that effective stress transfer takes place between epoxy matrix and buckypaper. Average tensile strength in buckypaper/epoxy films was found to be 17% greater than pristine epoxy films, suggesting homogeneous and consistent microstructure of buckypaper and good interfacial adhesion between constituent CNTs and resin. Lower modulus in randomly dispersed 1% by weight MWNT films can be attributed to nonhomogeneous distribution of MWNTs and formation of agglomerations because the use of surfactants and surface functionalization was avoided during the dispersion phase. Regions with agglomerated MWNTs may lack resin and this can lead to decrease in elastic modulus of the films.

Table 1. Mechanical Properties of Pristine, 1% by Weight MWNT, and Buckypaper/Epoxy Films

Specimen description	MWNT (% by weight)	Young's modulus (GPa)	Tensile strength (MPa)
Neat epoxy film	0	3.01 (0.22)	37.08 (2.58)
MWNT/epoxy film	1	2.72 (0.17)	38.60 (2.55)
Buckypaper/epoxy film	30	3.66 (0.26)	45.42 (3.99)

Note: Values in parentheses correspond to the standard deviation from five specimens.

Conclusion

The novel fabrication process presented in this paper enabled the production of large buckypapers with considerably shorter processing time. Structural homogeneity and stability along with uniformity in thickness were confirmed by SEM analysis and high porosity (81%) was achieved. The density of the buckypaper (0.42 g/cc) produced from this manufacturing process was close to buckypapers produced by the current vacuum filtration method. High weight fraction MWNT/epoxy films (30% by weight) could be fabricated and complete through-thickness resin impregnation was achieved. These films showed an average increase of 20% in tensile modulus compared with pristine epoxy films and 17% increase in tensile strength. Embedding buckypaper in GFRPs enabled real-time strain sensing with high sensitivity even for small strains, suggesting significant functionality of the buckypaper fabricated with the proposed technique. The ability to rapidly manufacture larger buckypapers can facilitate the implementation of multifunctional capabilities of CNTs at the industrial scale.

Acknowledgments

The authors gratefully acknowledge the support of this research by the Office of Naval Research (ONR; Grant N00014-14-1-0068) and program manager Mr. William Nickerson.

References

ARAMIS. (2012). *User's manual for 3-D image photogrammetry*, GOM mbH, Mittelweg, Braunschweig, Germany.

Ashrafi, B., Guan, J., Mirjalili, V., Hubert, P., Simard, B., and Johnston, A. (2010). "Correlation between Young's modulus and impregnation quality of epoxy-impregnated SWCNT buckypaper." *Composites, Part A*, 41(9), 1184–1191.

Bautista-Quijano, J. R., Avilés, F., Aguilar, J. O., and Tapia, A. (2010). "Strain sensing capabilities of a piezoresistive MWCNT-polysulfone film." *Sens. Actuators, A*, 159(2), 135–140.

Benlikaya, R., Slobodian, P., and Riha, P. (2013). "Enhanced strain-dependent electrical resistance of polyurethane composites with embedded oxidized multiwalled carbon nanotube networks." *J. Nanomat.*, 2013(2013), 327597.

Chen, X., et al. (2008). "Mechanical and thermal properties of epoxy nanocomposites reinforced with amino-functionalized multi-walled carbon nanotubes." *Mater. Sci. Eng. A*, 492(1–2), 236–242.

Cheng, Q., Bao, J., Park, J., Liang, Z., Zhang, C., and Wang, B. (2009). "High mechanical performance composite conductor: Multi-walled carbon nanotube sheet/bismaleimide nanocomposites." *Adv. Funct. Mater.*, 19(20), 3219–3225.

Chu, H., Zhang, Z., Liu, Y., and Leng, J. (2014). "Self-heating fiber reinforced polymer composite using meso/macropore carbon nanotube paper and its application in deicing." *Carbon*, 66, 154–163.

Cooper, S. M., Chuang, H. F., Cinke, M., Cruden, B. A., and Meyyappan, M. (2003). "Gas permeability of a buckypaper membrane." *Nano Lett.*, 3(2), 189–192.

Dharap, P., Li, Z., Nagarajaiah, S., and Barrera, E. V. (2004). "Nanotube film based on single-wall carbon nanotubes for strain sensing." *Nanotechnology*, 15(3), 379–382.

Dieze-Pascual, A. M., Guan, J., Simard, B., and Gomez-Fatou, M. A. (2012). "Poly(phenylene sulphide) and poly(ether ether ketone)

composites reinforced with single-walled carbon nanotube buckypaper: II–Mechanical properties, electrical and thermal conductivity." *Composites, Part A*, 43(6), 1007–1015.
Dumée, L. F., et al. (2010). "Characterization and evaluation of carbon nanotube Bucky-Paper membranes for direct contact membrane distillation." *J. Membr. Sci.*, 351(1–2), 36–43.
Fu, X., Zhang, C., Liu, T., Liang, R., and Wang, B. (2010). "Carbon nanotube buckypaper to improve fire retardancy of high-temperature/high-performance polymer composites." *Nanotechnology*, 21(23), 235701.
Iijima, S. (1991). "Helical microtubules of graphitic carbon." *Nature*, 354(6348), 56–58.
Islam, M. F., Rojas, E., Bergey, D. M., Johnson, A. T., and Yodh, A. G. (2003). "High weight fraction surfactant solubilization of single-wall carbon nanotubes in water." *Nano Lett.*, 3(2), 269–273.
Kang, I., Schulz, M. J., Kim, J. H., Shanov, V., and Shi, D. (2006). "A carbon nanotube strain sensor for structural health monitoring." *Smart Mater. Struct.*, 15(3), 737–748.
Lin, C. (2005). "Investigation and characterization of SWNT buckypaper manufacturing process." M.S. thesis, Dept. of Industrial and Manufacturing Engineering, Florida State Univ., Tallahassee, FL.
Liu, Q., Li, M., Wang, Z., Gu, Y., Li, Y., and Zhang, Z. (2013). "Improvement on the tensile performance of buckypaper using a novel dispersant and functionalized carbon nanotubes." *Composites, Part A*, 55, 102–109.
Lopes, P. E., et al. (2010). "High CNT content composites with CNT Buckypaper and epoxy resin matrix: Impregnation behaviour composite production and characterization." *Compos. Struct.*, 92(6), 1291–1298.
Meng, C., Liu, C., and Fan, S. (2008). "Flexible carbon nanotube/polyaniline paper-like films and their enhanced electrochemical properties." *Electrochem. Comm.*, 11(1), 186–189.
Moerman, K., Holt, C., Evans, S., and Simms, C. (2009). "Digital image correlation and finite element modelling as a method to determine mechanical properties of human soft tissue in vivo." *J. Biomech.*, 42(8), 1150–1153.
Oliva-Aviles, A. I., Aviles, F., and Sosa, V. (2011). "Electrical and piezoresistive properties of multi-walled carbon nanotube/polymer composite films aligned by an electric field." *Carbon*, 49(9), 2989–2997.
Ounnunkad, S., et al. (2011). "Comparison of the electrochemical behaviour of buckypaper and polymer-intercalated buckypaper electrodes." *J. Electroanal. Chem.*, 652(1–2), 52–59.
Park, J. G., et al. (2009). "Electromagnetic interference shielding properties of carbon nanotube buckypaper composites." *Nanotechnology*, 20(41), 415702.
Pham, G. T., et al. (2008). "Mechanical and electrical properties of polycarbonate nanotube buckypaper composite sheets." *Nanotechnology*, 19(32), 325705–325708.
Rein, M. D., Breuer, O., and Wagner, H. D. (2011). "Sensors and sensitivity: Carbon nanotube buckypaper films as strain sensing devices." *Comput. Sci. Tech.*, 71(3), 373–381.
Sears, K., et al. (2010). "Recent developments in carbon vanotube membranes for water purification and gas separation." *Materials*, 3(1), 127–149.
Slobodian, P., Riha, P., Lengalova, A., Svoboda, P., and Saha, P. (2011). "Multi-wall carbon nanotube networks as potential resistive gas sensors for organic vapor detection." *Carbon*, 49(7), 2499–2507.
Tasis, D., Tagmatarchis, N., Georgakilas, V., and Prato, M. (2003). "Soluble carbon nanotubes." *Chem. Eur. J.*, 9(17), 4000–4008.
Thostenson, E. T., Ren, Z., and Tsu-Wei, C. (2001). "Advances in the science and technology of carbon nanotubes and their composites: A review." *Comput. Sci. Tech.*, 61(13), 1899–1912.
Veliky, K. B. (2014). "Cast forming of carbon nanotube networks using paraffin." Honors thesis, Dept. of Industrial and Manufacturing Engineering, Florida State Univ., Tallahassee, FL.
Vohrer, U., Kolaric, I., Haque, M. H., Roth, S., and Detlaff-Weglikowska, U. (2004). "Carbon nanotube sheets for the use as artificial muscles." *Carbon*, 42(5–6), 1159–1164.
Whitby, R. L. D., Fukuda, T., Maekawa, T., James, S. L., and Mikhalovsky, S. V. (2008). "Geometric control and tuneable pore size distribution of buckypaper and buckydiscs." *Carbon*, 46(6), 949–956.
Yeh, C. (2004). "Characterization of nanotube buckypaper manufacturing process." M.S. thesis, Dept. of Industrial and Manufacturing Engineering, Florida State Univ., Tallahassee, FL.
Yekani Fard, M., Liu, Y., and Chattopadhyay, A. (2012a). "Analytical solution for flexural response of epoxy resin materials." *J. Aerosp. Eng.*, 10.1061/(ASCE)AS.1943-5525.0000133, 395–408.
Yekani Fard, M., Liu, Y., and Chattopadhyay, A. (2012b). "Characterization of epoxy resin including strain rate effects using digital image correlation system." *J. Aerosp. Eng.*, 10.1061/(ASCE)AS.1943-5525.0000127, 308–319.
Yekani Fard, M., Raji, B., and Chattopadhyay, A. (2014a). "The ratio of flexural strength to uniaxial tensile strength in bulk epoxy resin polymeric materials." *J. Polymer. Test.*, 40, 156–162.
Yekani Fard, M., Sadat, S. M., Raji, B., and Chattopadhyay, A. (2014b). "Damage characterization of surface and sub-surface defects in stitch-bonded biaxial carbon/epoxy composites." *Compos. Part B*, 56, 821–829.
Young, J. (2009). "Continuous buckypaper manufacturing process: Process investigation and improvement." M.S. thesis, Dept. of Industrial and Manufacturing Engineering, Florida State Univ., Tallahassee, FL.
Zhang, J., and Jiang, D. (2012). "Influence of geometries of multi-walled carbon nanotubes on the pore structures of Buckypaper." *Compos. Part A*, 43(3), 469–474.
Zhang, X. (2008). "Hydroentangling: A novel approach to high-speed fabrication of carbon nanotube membranes." *Adv. Mater.*, 20(21), 4140–4144.
Zheng, C., Qian, W., Yu, Y., and Wei, F. (2013). "Ionic liquid coated single-walled carbon nanotube buckypaper as supercapacitor electrode." *Particuology*, 11(4), 409–414.
Zhu, W., et al. (2010). "Buckypaper-based catalytic electrodes for improving platinum utilization and PEMFC's performance." *Electrochim. Acta*, 55(7), 2555–2560.